Title
DEVELOPMENT OF HIGH STRENGTH AND TOUGHNESS MICROCOMPOSITE HSLA FE/CR/MN/C STEEL WITH AND WITHOUT NB

Authors
Thomas, G.
Kim, J.K.
Manajlovic, D.

Publication Date
1987-12-01

LBL-23968 c.2

Lawrence Berkeley Laboratory
UNIVERSITY OF CALIFORNIA

Materials & Chemical Sciences Division

Presented at the International Conference
on HSLA Steels, Pittsburgh, PA,
November 3–5, 1987

Development of High Strength and Toughness Microcomposite HSLA Fe/Cr/Mn/C Steel with and without Nb

G. Thomas, J.K. Kim, D. Manojlovic
and R. Milovic

December 1987

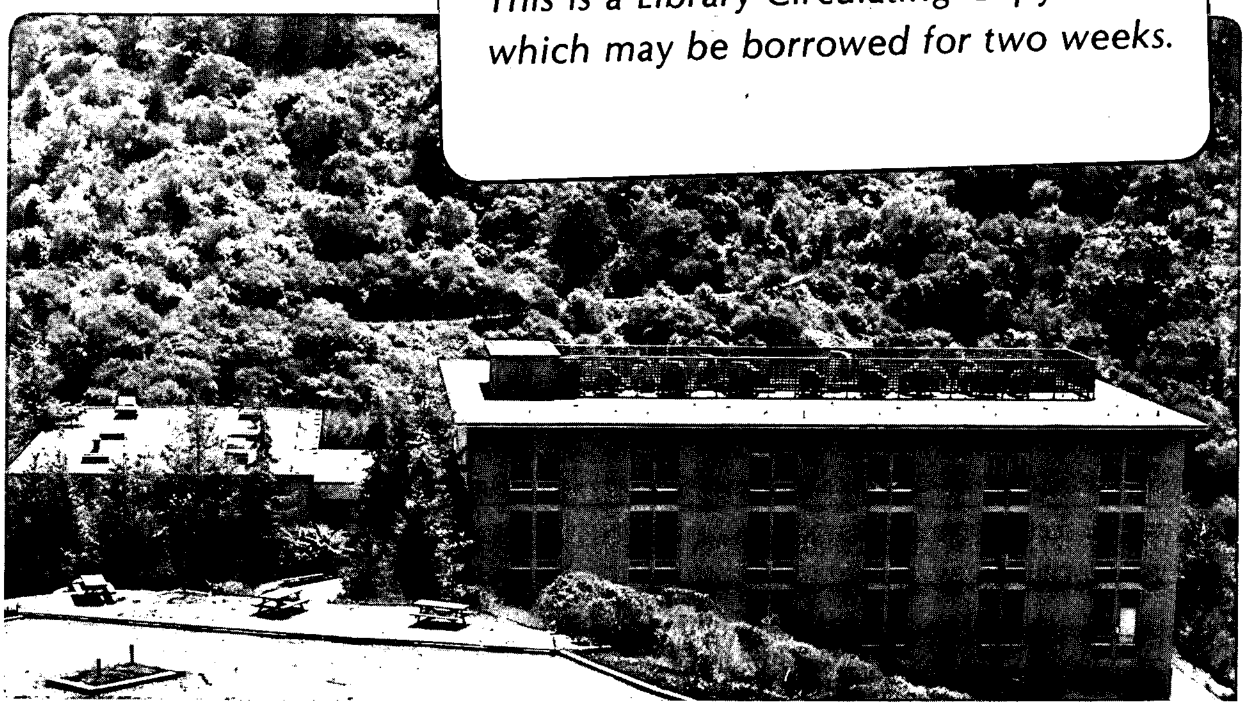

Prepared for the U.S. Department of Energy under Contract DE-AC03-76SF00098

DEVELOPMENT OF HIGH STRENGTH AND TOUGHNESS

MICROCOMPOSITE HSLA Fe/Cr/Mn/C STEEL

WITH AND WITHOUT Nb +

G. Thomas*, J.K. Kim**, D. Manojlovic***, and R. Milovic***

* Professor, Dept. of Materials Science and Mineral Engineering
University of California; Materials and Chemical Science
Division, and Scientific Director, National Center for
Electron Microscopy, Lawrence Berkeley Laboratory
Berkeley, CA 94720

** Dept. of Materials Science and Mineral Engineering
University of California, Berkeley, CA 94720

*** Boris Kidric Steel Works, Ferrous Metallugy Institute
Niksic, Yugoslavia

+ Paper presented at the International Conference
on HSLA Steels, Pittsburgh Pa, Nov. 3-5, 1987

Abstract

Microcomposite steels have been designed to consist of fine packet martensite and interlath austenite films in order to attain mechanical and corrosion properties with superior combinations of strength, fracture toughness, and formability in certain conditions . In an effort to improve these properties for on-line production in a hot mill for rounds and plates, modifications with niobium have been investigated and the CCT diagrams determined. The addition of niobium has achieved grain refinement without destroying the microcomposite morphology of packet martensite and austenite. Comparisons of properties, structure and processing are presented.

Introduction

In a continuing program on alloy design the principles of microcomposite structures are utilized to achieve superior combinations of mechanical properties, e.g., strength and fracture toughness. In the particular class of HSLA steels discussed here, the composite consists of fine grained packet lath martensites in which the laths are surrounded by thin films of austenite at about 5 vol.%. These structures have been optimized by developing Fe/Cr/Mn/C compositions and which maintain Ms>300°C to obtain autotempering, on cooling from above Ac_3. The present aspect of the research, is concerned with leaner Cr compositions (i.e.,1-2%) than those described previously(1), and to develop these microstructures on line in a steel plant by controlled hot rolling and accelerated cooling. However, with these alloys due to some reduction in hardenability rapid quenching rates of the order of 40°C/sec or faster is often required depending on final product thickness, in order to produce the desired packet martensite and to avoid carbide precipitation or other unwanted decomposition products during the quench. Thus in principle high strength, tough, plates as an example can be made directly on-line without necessarily requiring subsequent tempering. This method can provide economical advantages. However, in actual plant operation such rapid quenching rates are difficult to achieve and require enormous quantities of water. Thus, in the present work a Fe/2% Cr/1.2% Mn/0.25% C steel modified with 0.02%Nb has been developed in order to decrease the stringent quenching conditions and to increase hardenability whilst at the same time permitting achieving a fine austenite grain size during controlled hot rolling. The usual microalloying principle used for low carbon steels, by controlled rolling, usually below the austenite recrystallization temperature, is to reduce grain size by forming microalloyed carbides or carbonitrides at ferrite grain boundaries, so reducing grain growth(2). The resultant steels show excellent Charpy (crack initiation) toughness but because of the grain boundary precipitates often give poor K_{1C} toughness values i.e., poor crack progagation resistance (3). In the present scheme a different approach is used whereby the controlled rolling is done by finishing just above the austenite recrystallization temperature to produce a fine grained austenite which is then directly quenched to produce the desired microcomposite packet martensite-austenite. These comparative approaches are schematically shown in Fig.1.

As illustrated in Fig.2(a), the experiments have been done to investigate the effect of finishing rolling temperature and cooling rates on the tensile and Charpy fracture properties in the as-cooled condition, and also after subsequent tempering. The latter is already known to be optimum in the range 200-250°C and to avoid temper martensite embrittlement.(4-7). In a separate program interrupted accelerated cooling below Ms is also being investigated but will not be reported here.

A further processing route has been investigated in which the steels are controlled rolled (as in Fig. 2(b)), followed by normalizing rather than quenching, for which Nb additions may not be necessary. This processing produces a fine grained, bainitic or pearlitic structure, which can be easily and rapidly spheroidized so as to produce a cold formable product which can be subsequently quenched and tempered to achieve the same strong-tough microcomposite structure as indicated above

Experimental

The experimental alloys were vacuum melted to a 30 Kg ingot and subsequently forged to a 75 mm thick, 75 mm wide and 330 mm long billet. This was then homogenized at 1200°C for 24 hours in a vacuum furnace before cooling. The compositions given in Table

1 were measured after homogenization. Billets were cut into 40 mm thick, 38 mm wide and 76 mm long blanks, into which thermocouples were embedded to read the exact temperature during rolling. They were austenitized at 1200°C for 75 minutes in a horizontal furnace. Controlled rolling was conducted on the austenitized blanks as shown in Fig.2(a). The first rolling of 30 % reduction was done at 1100°C. The second finishing rolling was done at 950°C, 900°C and 850°C, respectively with the same reduction of 45 %. The cooling rate was also changed by dipping into water or agitated oil and by releasing in the air after controlled rolling. Isothermal tempering treatments were done at 200°C and 250°C.

Standard ASTM size specimens were used to measure the Charpy V-notch impact energy (the long axis of the test specimens was parallel to the rolling direction , and the base of the notch was perpendicular to the surface). Testing was conducted with a 224 ft-lb capacity impact machine at room temperature. Broken impact specimens were then examined for fractography in a scanning electron microscope operated at 25 Kv. The 31.5 mm gauge round tensile specimens were pulled at cross head speed of 0.3 mm/min at room temperature.

Microstructural examinations were conducted by optical and transmission electron microscopy (TEM) techniques. Thin foils for TEM were obtained from the broken impact specimens. Slices of about 500 μm were cut longitudinally with a 800 μm thick abrasive wheel under flood cooling and ground down to about 125 μm. 3 mm discs were cut off from these slices by mechanical punching and then carefully sanded down to about 50 μm and then electropolished in a twin jet electropolishing appparatus at -2°C in a perchloric acid - ethanol - glycerol solution at a voltage range of 12 to 15 volts and current range of 18 to 20 milliamperes. Transmission electron microscopy and diffraction were done on a Philips EM 301 Microscope operated at 100 Kv.

Continuous cooling transformation diagrams were obtained by the dilatometry method using various cooling rates.

Results

A. Mechanical Properties

The mechanical properties of the base quaternary and niobium bearing alloys are summarized in Tables 2 and 3. Tensile strength variations depended on finish rolling temperatures and cooling methods as is plotted in Fig. 3. As can be seen, the tensile strength of niobium bearing steels tends to show lower values than the alloy steel without niobium. However the differences are not significant in terms of general property requirements. Fig. 4 shows the comparison of Charpy impact energies of the two different steels. The niobium bearing steel shows a great improvement in impact toughness compared with the non-Nb quaternary alloy by about 15 joules. This is attributed to the effect of niobium on grain refinement as shown in Fig. 5. Finish rolling at 850°C shows a substantial decrease in Charpy impact energy because of rolling below the recrystallization temperature. Tempering at 200°C also contributes to the increment of Charpy impact energy. Therefore, a great improvement in impact toughness based on this simple experimental controlled rolling schedule can give the possibility of obtaining higher impact toughness by arranging a controlled rolling schedule in actual production without conducting any subsequent temper treatment.

Fig. 6 shows the effect of niobium on the ductility of ultra high strength microcomposite microalloy steel. Niobium also contributes to improve the ductility.

B. Microstructure

The microstructure of the present microcomposite microalloy steel is typical of that of packet martensites, now well described in the literature(1,4). These packets consist of parallel dislocated laths, thin films of interlath retained austenite and autotempered intralath carbides. A typical example of these features is given in Fig. 7. Tempering at 250°C does not change this microstructure appreciably. Retained austenite still exists (untransformed) at the lath boundaries as shown in Fig. 8.

C. Fractography

The change in the impact values can be explained by studying the fracture surface of the specimens using a scanning electron microscope. Fig. 9 shows the dimpled ductile fracture containing smaller dimples produced by autotempered carbide particles in the controlled rolled and as-quenched niobium bearing steel. Fig. 10 shows also the dimpled ductile fracture of niobium bearing steel temper treated at 200°C. Fig. 11 is an example of the cleavage surface of air cooled niobium steels which show very low Charpy impact values (Tables 2 and 3, Fig. 4).

D. Continuous Cooling Transformation Diagram

The continuous cooling transformation diagrams for the quarternary base alloy and the niobium bearing alloy are shown in Fig. 12. It is seen that niobium exerts a retarding role in the transformation of austentite to ferrite and bainite. This hardening effect of niobium makes possible the manufacture of ultra high strength and toughness microcomposite microalloy steel in on-line production because it removes the restriction of very high cooling rates which would otherwise be needed to obtain autotempered packets of lath martensite with retained austenite.

E. Cold Formability and Heat Treatment

The mechanical properties of the alloys described above appear to have attractive potential for applications involving cold forming, (welding) and final heat treatment of finished parts, that is, for products that cannot be produced directly on-line by hot rolling and accelerated cooling. Such examples include fasteners, chains, etc., in which bar stock are processed conventionally by spheroidizing, cold forming, (welding if needed) and final heat treatment, so as to attain the desired properties. In this case the role of niobium is less critical although it is still useful for grain refinement. The results presented here refer only to the non-niobium containing steel.

Since the carbides formed from the air cooled, rolled samples are of the M_3C type (mainly Fe_3C but may contain some Cr) these carbides can be rapidly spheroidized by only a couple of hours annealing below Ac_1. The Ac_1, and Ac_3 temperatures are 760°C and 823°C, respectively. In fact 2 hours at 720°C is adequate (as compared to perhaps 10 hours or more for alloyed steels such as boron containing steels). A typical micrograph is shown in Fig. 13. There are few interlath or intergranular plate-shaped carbides which would impair the subsequent cold formability. The prior austenite grain size was 7-8.

The average mechanical properties after spherodizing are, yield strength (0.2% proof) 515 N/mm^2, tensile strength 650 N/mm^2, Brinnel hardness 217, total tensile elongation 25 % with 75 % reduction in area.

The cold forming capabilities of the spheroidized steel are illustrated by the drawing results in Figs. 14 and in the micrograph of Fig. 15. This figure shows bars of initial diameter 16 mm, drawn to 14.3 mm, 12.4 mm, 11.3 mm and 10.1 mm respectively, followed by upset cold forging down to 1/3 and 1/6 of the initial height (1.5 x dia.). No cracking was detected. Furthermore after such cold forming, the steel is easily welded in the conventional way. An example for chains produced by cold forming the links, and pressure resistance welding is shown in Fig. 16. Following these operations, heat treatment of the steel is optimized by solution treating at 900°C followed by water quenching (Ms is 400°C) and tempering for 1 hr. at 225°C. Typical ASTM grain sizes are 7-8, depending on the initial grain size from the bar production.

The variation of mechanical properties with post forming heat treatments are summarized in Fig. 17. Clearly a range of properties is available. One attractive example for 900°C austenitizing and 1 hr. at 225°C temper is yield strength of 1250 N/mm^2, tensile strength of 1550 N/mm^2 at R_c of 44-48 and C_v of 50 joules (20°C) and 25 joules (-50°C).

The final microstructure is as shown in Fig. 18,viz, a microcomposite of tempered intralath carbides (M_3C) in dislocated packet lath martensite with the laths surrounded by thin films of untransformed austenite as is also obtained by direct processing (Fig.7,8). As has been shown earlier (5), these steels suffer from temper martensite embrittlement after tempering in the range 300°C-400°C depending on composition (e.g., Fig.19). This effect is due to decomposistion of the austenite into interlath carbides giving a brittle structure similar to bainite. At higher temperatures spheroidization occurs with a gain in Charpy toughness but a loss in strength (analagous to the data in Fig. 17).

Discussion

A. Controlled Rolling Steels

As is clear from the SEM example of Fig. 5, the main effect of the niobium compared to the non-niobium bearing alloy, is to provide austenite grain refinement for a given processing procedure. The exact machanism of this refinement is not known but it seems clear that it is not due to precipitation at the prior austenite grain boundaries, since no precipitates have been detected within the untransformed austenite films neither has niobium been detected after careful x-ray microanalyses were done using an intense, coherent field emission electron source. Clearly in some way niobium must exert a drag on the boundaries so reducing grain growth after recrystallization. It is to be expected that due to the higher solubility of niobium in austenite, this element should be concentrated in this phase. In "conventional" microalloyed low carbon steel the transformation of austenite to ferrite suddenly lowers the solid solubility and hence increase the tendency for Nb(CN) to form at the ferrite grain boundaries. No Nb(CN) precipitates were detected in the martensite phase either but investigations are still proceeding on this point since very little is known regarding hot rolling effects on precipitation in these microalloyed class of steels.

The tables of properties (Tables 2 and 3) shows that niobium has no significant effect on the yield and tensile strengths but it does increase tensile ductility and Charpy toughness. The main effect of finishing temperature is to optimize grain refinement but it is important not to finish at too low a temperature which could generate pro-eutectoid decomposition products and thereby lower toughness. As shown in Tables 2 and 3, the Charpy values are increased, as expected, by the tempering treatment following cooling from the finish temperature. However, the as-quenched properties are still promising for certain applications such as wear plate in mining.

As yet comprehensive data have not been obtained on the K_{1C} toughness, preliminary results on optimally rolled (900°C finish roll temperature), water-quenched and tempered samples give K_C (i.e., not ideal plane strain values) of close to 150 MPa $m^{1/2}$ which in combination with a yield strength of 1200 MPa and Charpy values of about 50 joules (20°C) are quite exciting.

Although Nb provides improved hardenability, the cooling rates needed to achieve the desired microcomposite packet martensite-retained austenite morphology may still be too rapid in commercial practice to ensure optimum autotempering (as evidenced by the tempering results) by direct cooling. Thus for highest toughness post quenching tempering of on-line hot mill products will be required. However, interrupted cooling experiments indicate that it is possible to achieve superior toughness at high strength levels without an extra tempering step corresponding to all treatments.

B. Cold Formability

The ease of spheroidizing, excellent cold formability and excellent mechanical properties after heat treatment also illustrates the potential of these microcomposite steels for many applications besides on-line rolled finished products. The absence of alloy carbides allows rapid spherodizing, involving a factor of 4 to 5 times savings on time (2 hrs. compared to typically 10 hrs. for B containing steels). The versatility of these steels represents a wide range of potential applications for only one composition.

Summary

This research has indicated some benefits of small additions of niobium to HSLA lath martensite-austenite composite steels for on-line controlled rolling and accelerated cooling processing routes applicable to plates (about 20 mm thickness) and other products. Futher research will be aimed at understanding the effects of niobium in more detail and this will include if possible the influence of rolling conditions on the CCT diagram (Fig. 12). The non-niobium containing steels can be processed in a similar manner, but without requiring on-line quenching to provide an easily spheroidizable steel for cold forming and welding operations, finishing in the usual manner with a quench temper treatment to achieve superior combinations of mechanical properties

Acknowledgments

The non-niobium steels were produced and the cold forming processing was done at the Boris Kidric Steel plant. The niobium containing alloy was kindly provided by Pohang Steel Co., which supports J.K. Kim (Ph.D. candidate). This work was supported by the Director, Office of Energy, Office of Basic Energy Sciences, Division of Materials Science of the United States Department of Energy under Contract No. DE-AC03-76SF00098.

References

1. B. V. N. Rao and G. Thomas, Met. Trans. A, 1980, Vol. 11A, 441-457.

2. T. Tanaka, Int. Met. Reviews, 1981, No. 4, 185-212.

3. R. O. Ritchie, B. Francis, and W. L. Server, Met. Trans. A, 1976, Vol., 7A, 831-838.

4. M. Sarikaya, A.K. Jhingan, and G. Thomas, Met. Trans., A, 1983, Vol.,14A, 1121-1133.

5. G. Thomas, Met.,Trans. A, 1978, Vol. 9A, 439-450.

6. R. M. Horn and R. O. Ritchie, Met. Trans. A, 1978, Vol. 9A, 439-450.

7. J. A. McMahon and G. Thomas, Proceedings of the International Conference on the Microstructure and Design of Alloys, Inst. of Metals, London, 1973, Vol. 1, 180-184.

Table 1. Alloy Compositions

Alloy	C	Mn	Cr	Nb	Si	P	S
Non Nb Steel	0.26	1.20	1.99	-	0.14	0.012	0.015
With Nb Steel	0.24	1.21	1.98	0.02	0.046	0.006	0.004

Table 2. Mechanical Properties of Fe/0.25% C/1.2% Mn/2.0% Cr

First Rolling Temp(°C)/Red(%)	Second Rolling Temp(°C)/Red(%)	Tempering Temp(°C)	YS (MPa)	UTS (MPa)	Elongation Total(%)	Charpy Impact Energy(J)
1100/30	950/45	As-WQ	1208	1630	12.6	33
"	"	200				38
"	"	250	1236	1505	14.7	35
"	"	As-OQ	1139	1608	15.4	29
"	"	200				33
"	"	250	1236	1498	16.8	31
"	"	Air Cool	842	1188	15.4	4
"	900/45	As-WQ	1374	1601	13.3	29
"	"	200				35
"	"	250	1111	1456	13.3	34
"	"	As-OQ	1208	1601	16.8	26
"	"	200				31
"	"	250	1236	1519	15.4	29
"	"	Air Cool	739	1111	18.2	4
"	850/45	As-WQ	1456	1769	10.2	15
"	"	200				19
"	"	250	1312	1656	15.4	19
"	"	As-OQ	1236	1760	15.4	15
"	"	200				24
"	"	250	1284	1637	14.7	22

Table 3. Mechanical Properties of Fe/0.25% C/1.2% Mn/2.0% Cr/0.02% Nb

First Rolling Temp(°C)/Red(%)	Second Rolling Temp(°C)/Red(%)	Tempering Temp(°C)	YS (MPa)	UTS (MPa)	Elongation Total(%)	Charpy Impact Energy(J)
1100/30	950/45	As-WQ	1139	1540	16.1	46
"	"	200				52
"	"	250	1188	1485	16.1	41
"	"	As-OQ	1126	1512	16.1	42
"	"	200				46
"	"	250	1208	1485	16.8	41
"	"	Air Cool	842	1091	19.6	4
"	900/45	As-WQ	1138	1560	16.8	38
"	"	200				46
"	"	250	1188	1540	16.8	35
"	"	As-OQ	1160	1519	16.8	48
"	"	200				54
"	"	250	1160	1485	15.4	42
"	850/45	As-WQ	1160	1540	14.7	35
"	"	200				41
"	"	250	1340	1512	14.0	31

<u>Figure Captions</u>

Fig. 1. Schematic to show processing between conventional and microcomposite microalloying.

Fig. 2. Controlled rolling schedule (a) and cold forming process (b).

Fig. 3. Tensile strength variations of non-Nb steel and Nb-bearing steel vs. finish rolling temperature.

Fig. 4. Charpy impact energy variations of non-Nb steel and Nb-bearing steel vs. finish rolling temperature.

Fig. 5. Comparison of prior austenite grain sizes. Average sizes are 35 μm for non-Nb steel and 19 μm for Nb-bearing steel. Both of them are finish-rolled at 900°C.

Fig. 6. Total elongation variations of non-Nb steel and Nb-bearing steel vs. finish rolling temperature.

Fig. 7. Transmission electron micrographs of finish-rolled at 900°C and as-quenched Nb steel. Dark field image(RHS) shows the interlath austenite.

Fig. 8. Transmission electron micrographs of Nb steel finish-rolled at 900°C and temper-treated at 250°C. The carbides are {110} M_3C type.

Fig. 9. Scanning electron micrograph of Nb steel finish-rolled at 900°C and water-quenched. Fracture surface exhibits ductile fracture. Smaller dimples are produced by autotempered carbide particles.

Fig. 10. Scanning electron micrograph of Nb steel finish rolled at 900°C, water-quenched, and temper-treated at 200°C. It represents ductile fracture.

Fig. 11. Scanning electron micrograph of air-cooled Nb steel. Surface shows typical cleavage fracture.

Fig.12. CCT digrams of Fe/Cr/Mn/C steel with and without 0.02% Nb. Nb increases hardenability by exerting a retarding role in decomposition of austenite.

Fig. 13. Transmission electron micrograph of spheroidized cementite (2 hrs. at 720°C).

Fig. 14. Tensile and yield strengths vs. cold drawing(a) and ductility vs. cold reduction(b).

Fig. 15. Bars cold drawn from 16 mm diameter, upset forged to 1/3 and 1/6
of original height (=1.5 x diameter). No failure after 60% reduction.

Fig. 16. Chain made of non-Nb steel after cold forming process. Also shown is a cold headed bar e.g., for concrete ties(a). Cold headed screw made of non-Nb steel is shown(b).

Fig. 17. Mechanical properties of non-Nb steel, e.g., strength variation (a), total elongation(b) and Charpy impact energy(c). The material was austenitized at 900°C and water-quenched after cold forming.

Fig. 18. Transmission electron micrographs of Nb steel finish-rolled at 900°C and water-quenched.

Fig. 19. Transmission electron micrographs of interlath stringer type cementite decomposed from retained austenite tempered at 400°C.(a); Bright field image. (b); Dark field image of interlath stringer of cementite.

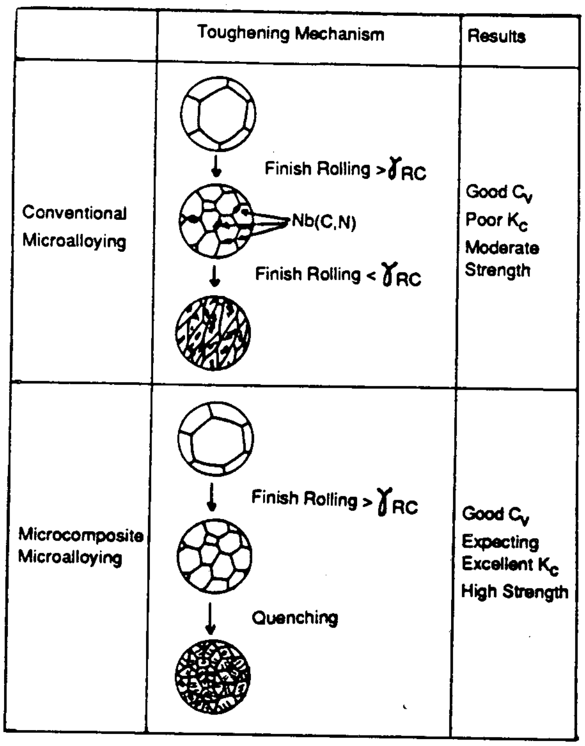

XBL 881-213

Fig. 1.

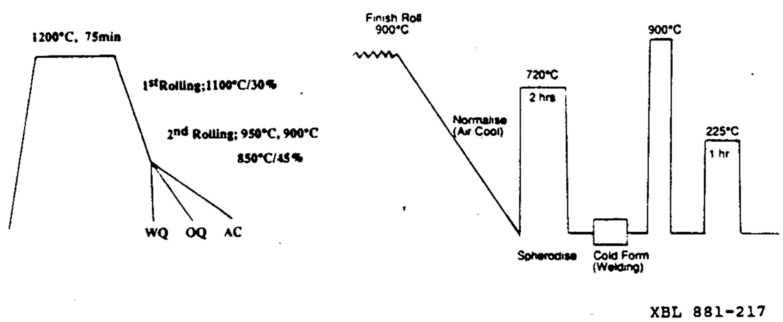

(a) (b)

Fig. 2

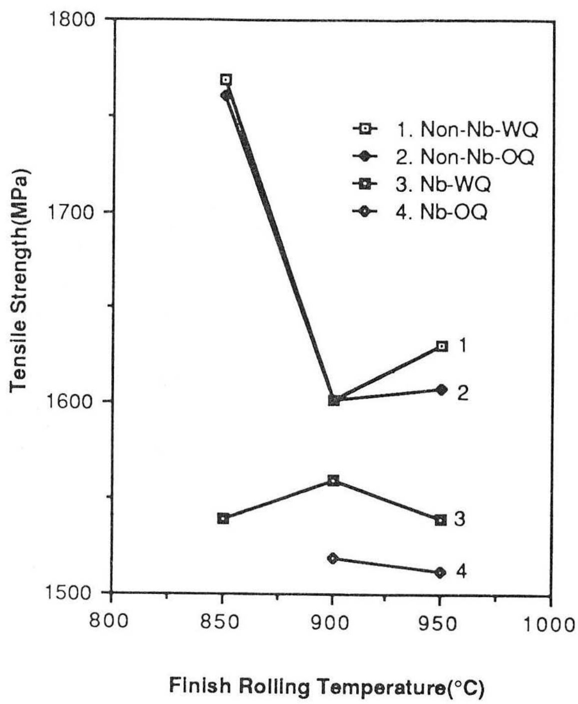

Fig. 3 XBL 881-215

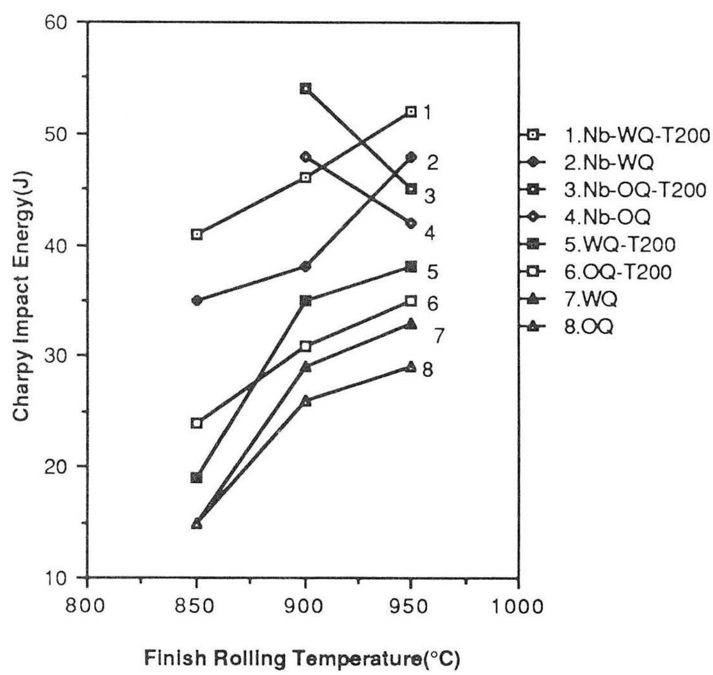

Fig. 4 XBL 881-216

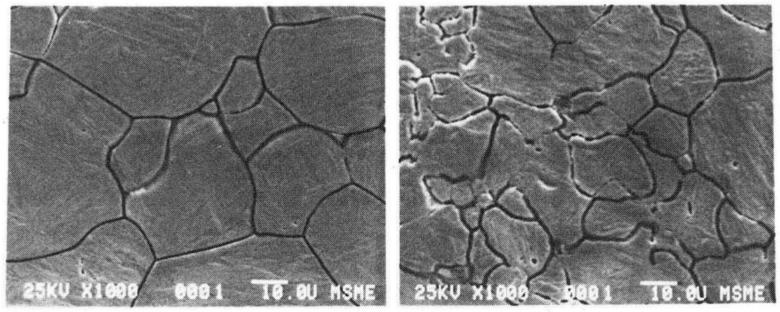

Prior Austenite Grain of Non-Nb Steel (ASTM Standard #7).

Prior Austenite Grain of Nb Steel (ASTM Standard #9).

XBB 870-9085

Fig. 5

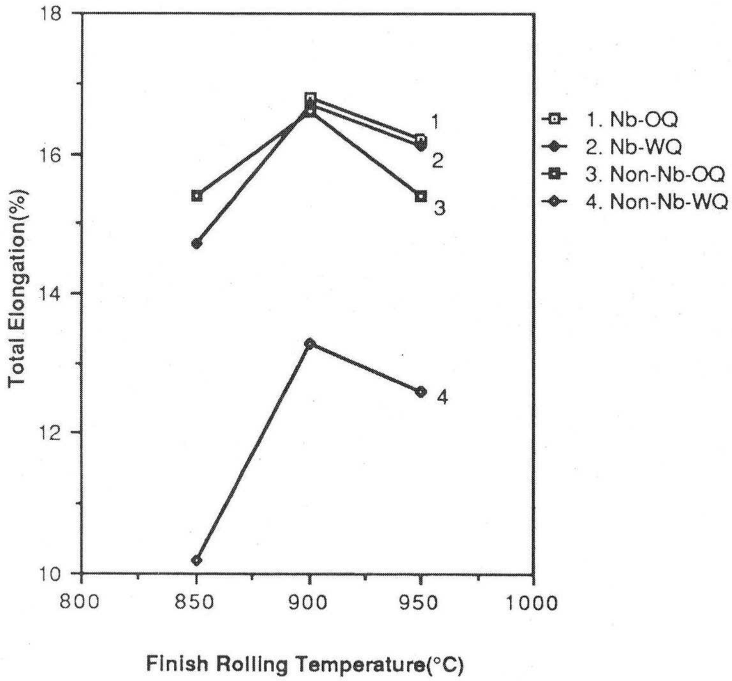

Fig. 6 XBL 881-214

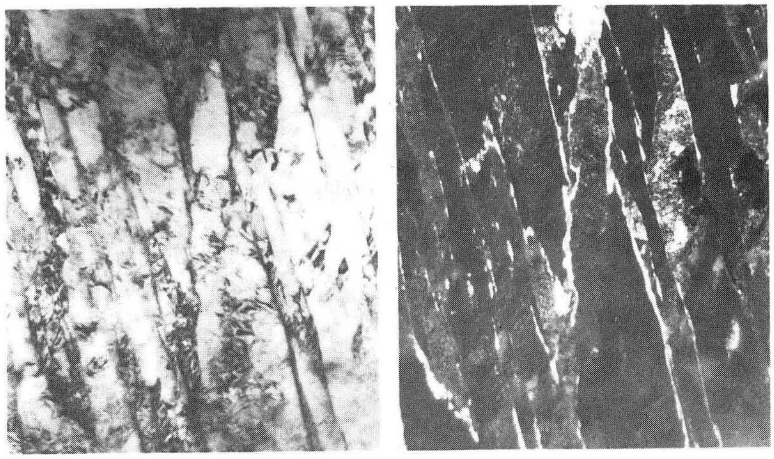

XBB 870-9092

Fig. 7

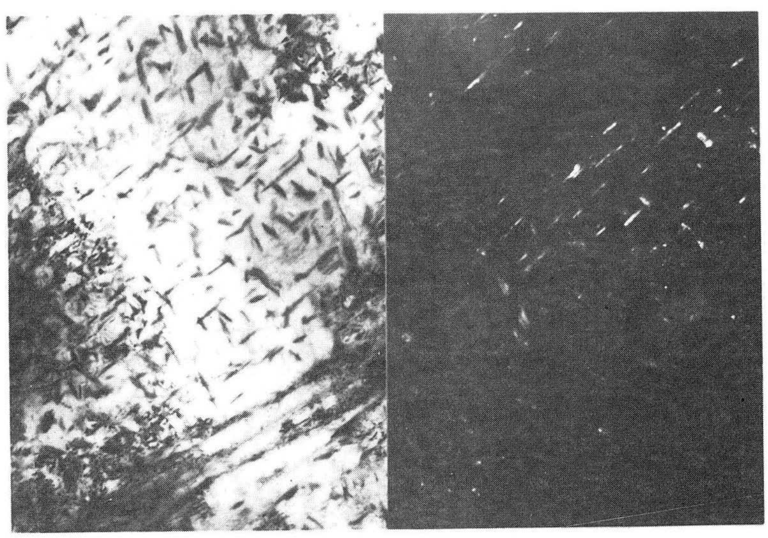

XBB 870-9091

Fig. 8

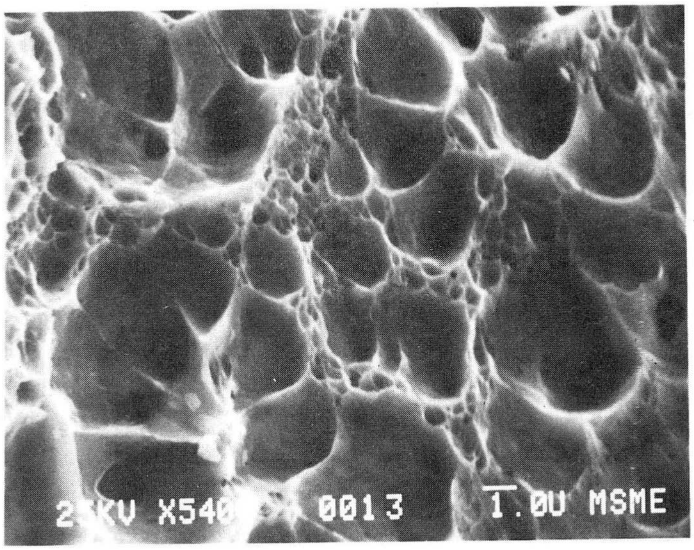

XBB 870-9087

Fig. 9

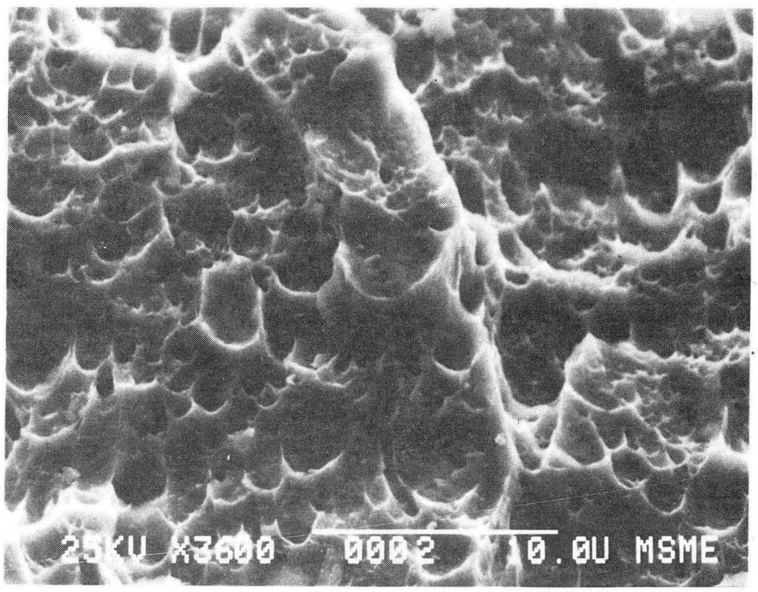

XBB 870-9088

Fig. 10

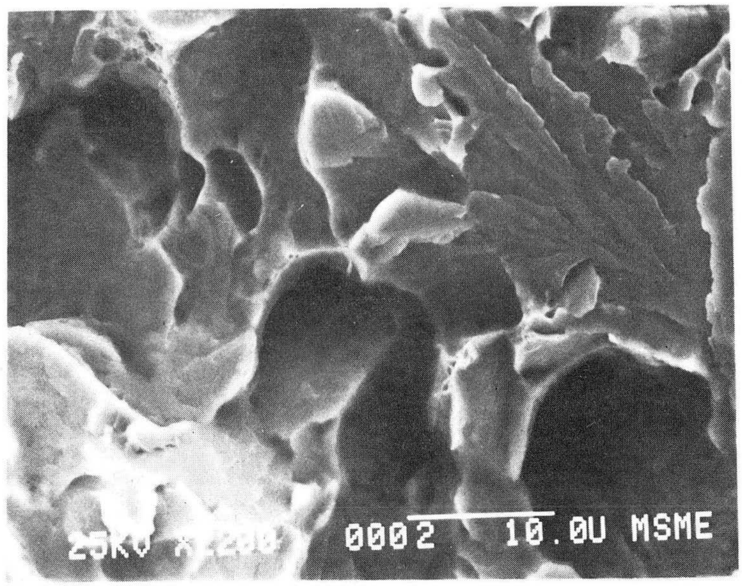

XBB 870-9086

Fig. 11

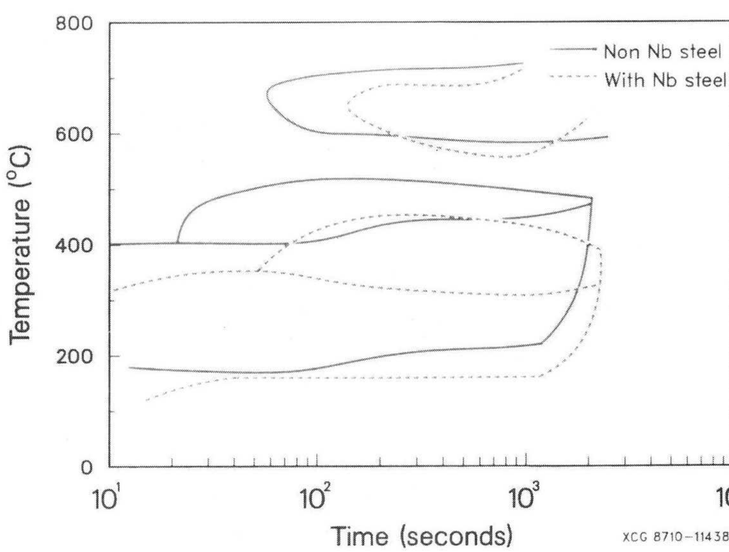

Fig. 12

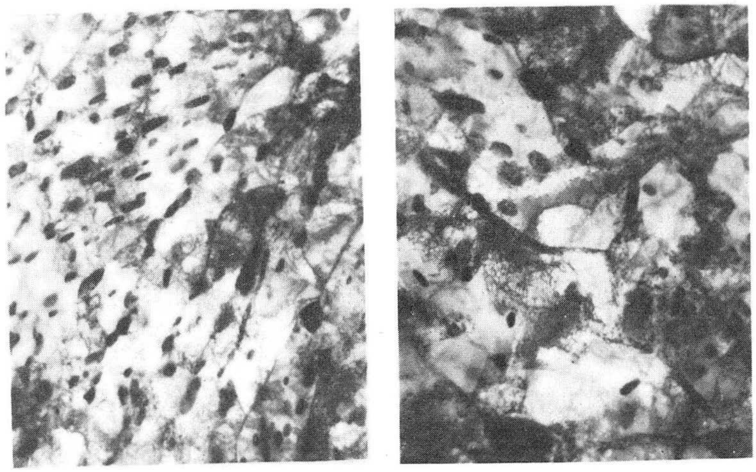

XBB 870-9089

Fig. 13

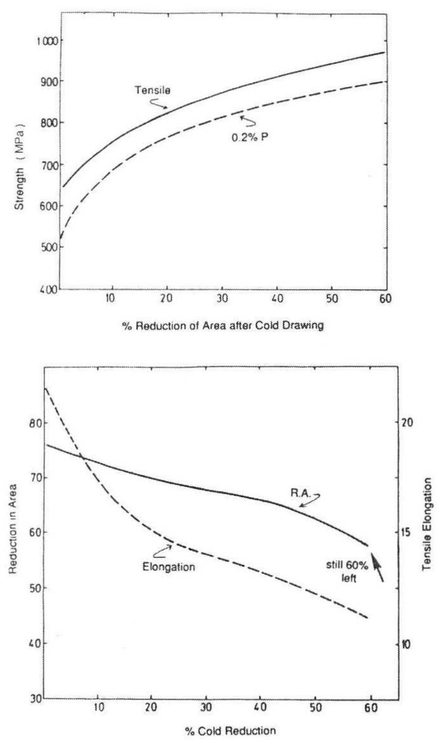

XBL 881-211

Fig. 14

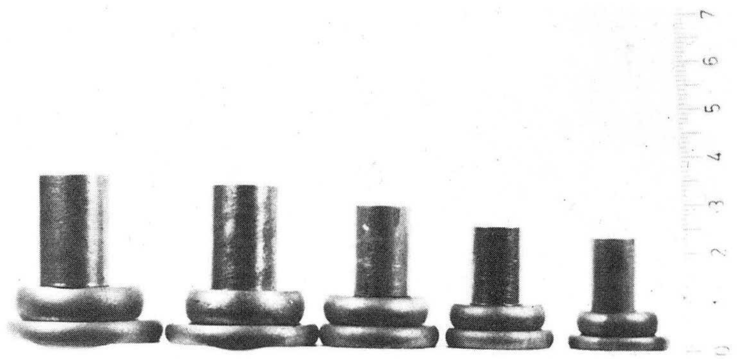

Bars Cold Drawn from 16mm diameter, Upset Forged to 1/3 and 1/6 of Original Height(=1.5xdiameter). No Failure after 60% Reduction. XBB 870-9093

Fig. 15

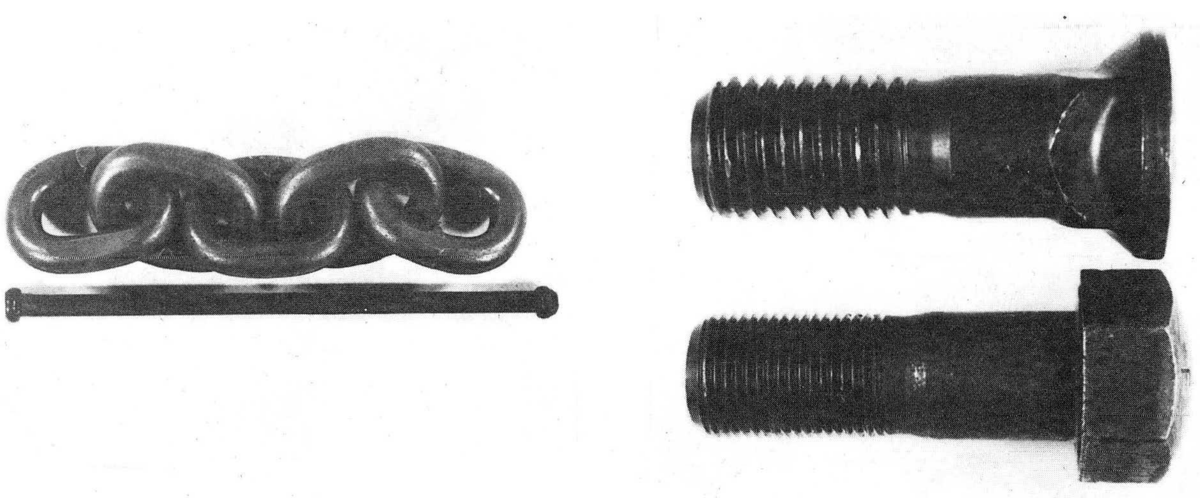

(a) (b)

Fig. 16

XBB 870-10666

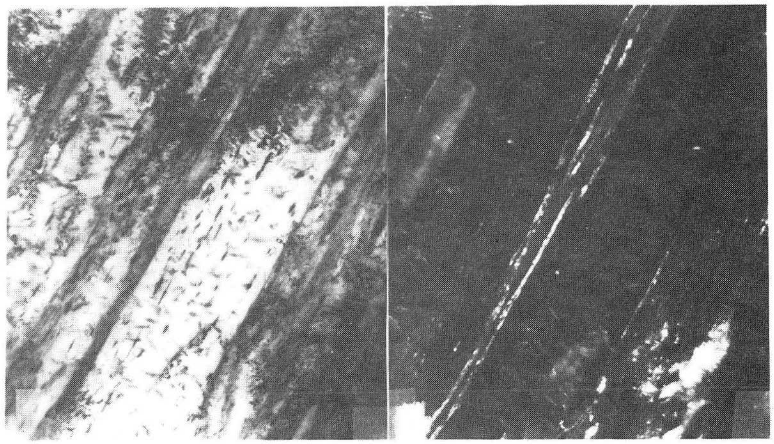

XBB 870-10610

Fig. 18

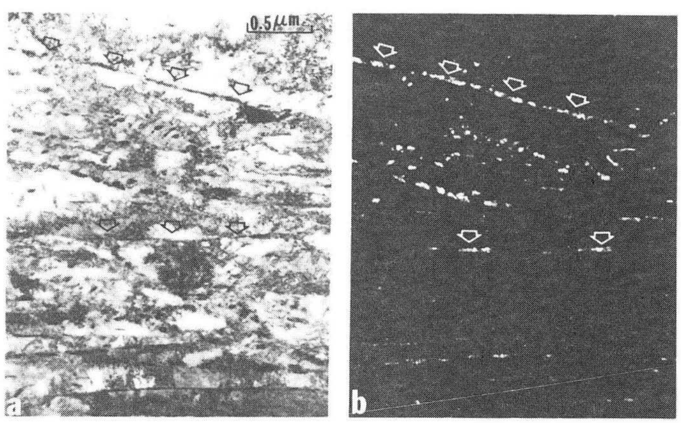

XBB 782-1178

Fig. 19

LAWRENCE BERKELEY LABORATORY
TECHNICAL INFORMATION DEPARTMENT
UNIVERSITY OF CALIFORNIA
BERKELEY, CALIFORNIA 94720